
STACKING VAE WITH GRAPH NEURAL NETWORKS FOR EFFECTIVE AND INTERPRETABLE TIME SERIES ANOMALY DETECTION

A PREPRINT

Wenkai Li^{1,2}, Wenbo Hu², Ning Chen¹, Cheng Feng³

¹ Dept. of Comp. Sci. & Tech., Tsinghua University

² RealAI, ³ Siemens AG, Beijing

liwk20@mails.tsinghua.edu.cn, i@wbhu.net

ningchen@tsinghua.edu.cn, cheng.feng@siemens.com

May 19, 2021

ABSTRACT

In real-world maintenance applications, deep generative models have shown promising performance in detecting anomalous events of entities from time-series signals collected from multiple sensors. Nevertheless, we outline two important challenges of leveraging such models for times-series anomaly detection: 1) developing effective and efficient reconstruction models and 2) exploiting the similarity and interrelation structures among the multivariate time series data channels. To address these challenges, in this paper we propose a stacking variational auto-encoder (VAE) model with graph neural networks for the effective and interpretable time-series anomaly detection. Specifically, we propose a stacking block-wise reconstruction framework with a weight-sharing scheme for the multivariate time series data with similarities among channels. Moreover, with a graph learning module, our model learns a sparse adjacency matrix to explicitly capture the stable interrelation structure information among multiple time series data channels for interpretable reconstruction of series patterns. Experimental results show that our proposed model outperforms the strong baselines on three public datasets with considerable improvements and meanwhile still maintains the training efficiency. Furthermore, we demonstrate that the intuitive stable structure learned by our model significantly improves the interpretability of our detection results.

Keywords time-series, anomaly detection, deep generative model, graph neural network

1 Introduction

Time-series anomaly detection is an important task with wide applications in real-world maintenance systems [1, 2]. It aims to automatically identify whether an anomaly occurs by monitoring one or multiple channels of given time-series data. Typical applications of time-series anomaly detection include intrusion detection [3], fraud detection [4], disease outbreak detection [5] and artificial intelligence for IT Operations (AIOps) [6]. For example, under the AIOps scenario, multiple sensors are deployed to monitor the operating indices of the running IT devices. These indices are regular and predictable when devices are running normally. Time-series anomaly detection methods can be employed to learn such normal patterns and then detect the system failures automatically.

Among various solutions, deep generative models (DGMs) are becoming increasingly popular in recent years [7, 8, 9] due to their strong ability to fit complex data in an unsupervised manner. In particular, DGMs build a reconstruction model for the normal data and often use data likelihoods as the evaluation criterion for the time series anomaly detection task. Although such methods have shown great promise, they are still insufficient to capture the rich structure information among multivariate time-series. For instance, Fig. 1 provides a typical example of a real-world time series normal data sample (the raw data of the A-3 instance from the SMAP dataset [10], which contains several

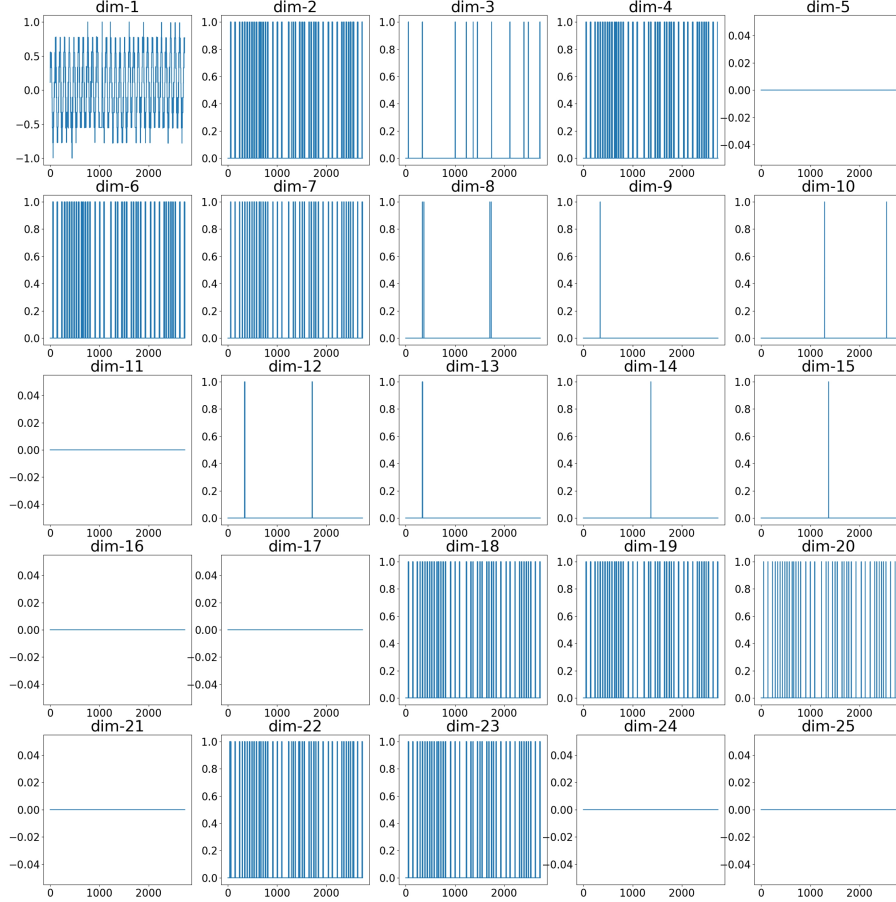


Figure 1: An illustration of the 25 channels in A-3 instance of the SMAP dataset used for model training. The training set is considered to contain only normal data. From the upper left corner in the first row, these channels are indexed by channel 1, 2, 3, . . . The channels can be roughly clustered into several groups according to their similarity. Moreover, there are strong interrelations among channels due to the location proximity of sensors and the correlations of measurements, which will be further exploited to build our efficient and interpretable time series anomaly detection model.

telemetry indicators of the global soil moisture and freeze-thaw state). We can see the clear similarities and interrelation structures among the multiple channels. These similarities and interrelation stem from the location proximity of sensors and the correlations of measurements and widely exist in various tasks, including moisture monitoring, health care, environmental monitoring, etc. The existence of such structures poses two challenges when building a deep generative model for effective and interpretable anomaly detection:

- **Reconstruction modeling challenge:** how to effectively build the reconstruction model for the multivariate temporal signals with similarities among channels?
- **Interrelation structure challenge:** how to exploit the structure information originated from the interrelation among the multiple channels?

For the *reconstruction modeling challenge*, one can build a *step-wise model* with an auto-encoder (AE) [11] or variational auto-encoder (VAE) [12] unit for every time step [7, 9, 13]. However, such a step-wise model may lead to overfitting on not only the normal data but also the unknown anomalies when training. An alternative way is to reconstruct the signals of multiple steps in one sliding window, i.e., the *block-wise reconstruction*. By building a block-wise reconstruction model, one can obtain the robust reconstructions from a more global view [8, 14, 15], leading to better robustness to the anomalous noise than the step-wise models. However, the block-wise reconstruction methods often adopt a larger network, which inevitably increases the cost of model training. To deal with this issue, the similarities among the multiple channels of time-series data need to be properly considered to benefit the anomaly detection task.

As for the *interrelation structure challenge*, the structure information is originated from the interrelations among the multiple channels and is essentially important for building an effective and interpretable deep generative model for the time series anomaly detection task. Generally the prior knowledge of the interrelation structure is hard to obtain in advance. The existing methods model the interrelation structure either in implicit neural networks or the probabilistic latent space, which are uninterpretable and unstable [7, 9, 15, 16]. The reasons will be detailed in Section 2.3.

In this paper, we propose a novel method to learn effective series patterns and interpretable structures for multivariate time-series anomaly detection. Towards the reconstruction modeling challenge, we propose a stacking block-wise reconstruction framework, which is to stack a single-channel block-wise VAE model with a weight-sharing technique for multivariate data with channel-level similarities. Regarding to the interrelation structure challenge, apart from the proposed reconstruction framework, our model learns a sparse adjacency matrix via a graph learning module from time series data in every channel. The learned graph can effectively extract stable structure information to achieve a more interpretable reconstruction process. Extensive experiments show that our method not only achieves the state-of-the-art time-series anomaly detection performance, which verifies the success on modeling time-series with channel-level similarities, but also learns the interpretable structure information via the graph learning module. Moreover, the training efficiency of our model is also shown via the training time of every epoch.

2 Background

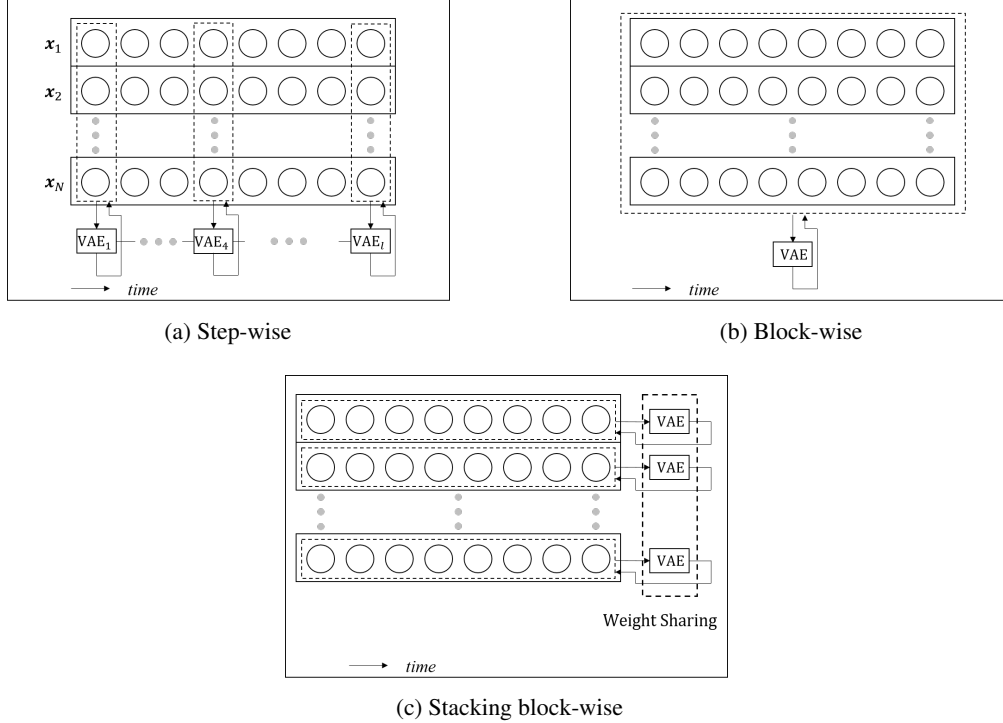


Figure 2: The architecture of deep generative models for times-series anomaly detection. Fig. 2a and Fig. 2b are for previous works. Fig. 2c is proposed in this paper. Here we use VAE as a representative to show its possible usage when reconstructing one slice $X \in \mathbb{R}^{N \times l}$.

In this section, we provide the background of time-series anomaly detection and deep generative models. We also introduce the related methods of graph learning and structure learning methods for time-series data.

2.1 Time-series Anomaly Detection

Given a multivariate time-series dataset $S \in \mathbb{R}^{N \times T}$, we denote the number of the channels as N and the length of the time-series as T . The goal of time-series anomaly detection is to find the anomalous points and segments among these T time steps. In practice, we use a sliding window to split the original multivariate time-series $S \in \mathbb{R}^{N \times T}$ into multiple slices with a pre-defined window size l : $X_l, X_{l+1}, \dots, X_t, \dots, X_T$. The slice X_t contains l multivariate observations

ranging from the time step $t - l + 1$ to t . Although the time-series data may have various types of anomalies, the anomalies can be detected by exploiting the normal patterns such as the trend and the seasonality [1]. If there is only one dimension for the time-series data S , i.e., $N = 1$, we call it univariate (or single-channel) time-series anomaly detection, and the anomaly detection models mainly explore the temporal dependency to identify abnormal patterns. When it comes to the multivariate data, i.e., $N > 1$, besides the temporal dependency of the time-series, we should also explore the channel-level interrelations, which usually remain stable when the monitored system is running normally, as the additional structure information for solving the anomaly detection task.

Supervised methods, such as deep neural networks and support vector machines, can be directly migrated to time-series anomaly detection by considering it as a classification task [17]. However, in practical scenarios the label scarcity and diversity of time-series anomalies prevent the further application of the supervised methods. Unsupervised anomaly detection methods are more commonly used than supervised ones. Traditional unsupervised anomaly detection methods, such as one-class SVM [18] and isolation forest [19], can be naturally applied to the time-series data with good interpretability. Apart from the traditional methods, generally, the existing unsupervised approaches based on neural networks can be classified into prediction-based methods and reconstruction-based methods. As an example of prediction-based methods, LSTM-NDT [10] firstly uses LSTM to perform time series forecasting and on this basis the nonparametric dynamic thresholding method is used on prediction errors to detect anomalies. For reconstruction-based methods, deep generative models have been widely adopted with fruitful progress, which is detailed in the following part.

2.2 Deep Generative Models for Time-Series Anomaly Detection

. Probabilistic methods are one of the most popular unsupervised methods for the time series anomaly detection task. They adopt the unsupervised generative modeling for the time-series and obtain the anomaly score according to the data point likelihoods [1]. In particular, the recent advances on deep generative models (DGM) (such as variational auto-encoder, VAE [12]), which leverage deep neural networks to dramatically increase the model capacity, have been widely applied to the time-series anomaly detection task. Generally, DGMs reconstruct the normal patterns of the raw input data and detect anomalies in an unsupervised fashion.

As stated in Section 1, there two general categories of DGMs — step-wise and block-wise methods, as illustrated in Fig. 2a and Fig. 2b respectively. Specifically, *step-wise approaches* use a recurrent neural network (RNN) cell to build the reconstruction model at each time step. For instance, LSTM-Encoder-Decoder [13] uses an LSTM cell to encode the multivariate time-series for each time step and then reconstructs the input series reversely in the autoencoder framework. LSTM-VAE [7] equips the LSTM cell in the VAE framework, showing VAE’s superiority of the probabilistic reconstruction in the continuous latent space. Then GGM-VAE [16] assumes a Gaussian mixture prior in the latent space to replace the uni-modal Gaussian assumption of VAE. OmniAnomaly [9] employs a stochastic recurrent neural network with stochastic variable connection and planar Normalizing Flows [20] to further describe non-Gaussian distributions of latent space. However, one common weakness of such step-wise methods is that they are prone to overfit both the normal data and the anomalies because of the strategy on building a reconstruction model on every time step.

To partly address the weakness of step-wise methods, *block-wise approaches* choose to reconstruct the time-series data of sliding windows block by block. For instance, Donut [8] is a single-channel anomaly detection model based on VAE with a modified ELBO (M-ELBO), missing data injection, and MCMC imputation techniques. [14] proposed the UnSupervised Anomaly Detection (USAD) for multivariate time-series, which introduced the adversarial training into the training procedure of a block-wise reconstruction model. The adversarial training amplified the reconstruction error of inputs so that the USAD model can detect the anomalies with small deviates. In general, block-wise methods have a more robust reconstruction mechanism. However, they often have a large size of model weights, and need more computation and data in order to train well for better capturing the series patterns. Overall, it is still a challenging task to build an effective reconstruction model for the multi-channel time series with similarities.

2.3 Graph Learning and Structure Learning for Time-Series

When it comes to the multivariate time-series data, one can use auto-regression methods with the other endogenous variables and build up a vector auto-regression (VAR) model [21]. The recurrent neural networks, such as LSTM [22], can be used to build deep learning models for multivariate time-series data. But in these recurrent deep models (also including the step-wise approaches [7, 9, 13]), the relationships among the channels are implicitly represented in the weights, resulting in the lack of interpretability. GGM-VAE [16] improves the model interpretability by assuming a Gaussian mixture prior in the latent space, but the structure information in the latent mixture space cannot correspond to the channel dimension. MSCRED [15] further uses the correlations between each pair of channels and this correlation

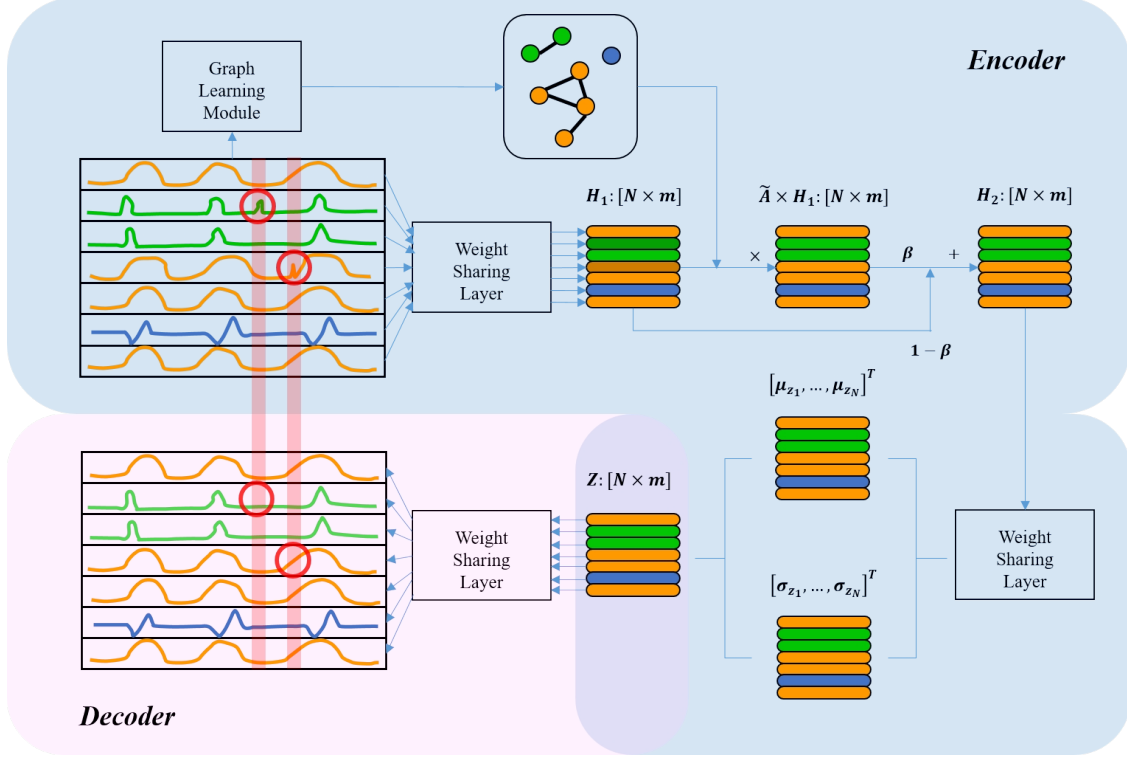


Figure 3: The architecture of StackVAE-G. Under the stacking block-wise reconstruction framework, the multivariate time-series data is encoded into the mid-latent feature H_1 . Then the single-channel VAE model is stacked with a weight-sharing Linear layer for multivariate time series data with channel-level similarities. Moreover, the channels are regarded as graph nodes and a graph neural network module is used to learn the interrelation among the channels.

matrix contains the structure information therein. However, MSCRED gives time-varying structures without considering the stable structure information under the normal state.

After evaluating the existing time-series anomaly detection models from structure learning perspective, we briefly introduce the specialized structure learning algorithms on multivariate time-series data. The prior knowledge for the structure information of the multivariate time-series is often unknown, so it is a challenge to model the interrelation among the multiple channels. This interrelation structure information can be derived from the feature sparsity and represented as graphs [23, 24]. Graphical lasso [25] transferred the structure learning problem to inverse covariance matrix estimation. More recently, [26] proposed a graph neural network module for learning the directed spatial dependency for the multivariate time-series forecasting tasks.

3 Methodology

We now present our proposed Stacking-VAE with Graph neural network (StackVAE-G) model, which is composed of two modules, a stacking block-wise VAE (StackVAE) and a graph neural network (GNN) module.

Fig. 3 shows the overall architecture of our model. Towards effective anomaly detection, StackVAE builds the reconstruction model by stacking single-channel reconstruction procedures with shared weights to exploit the channel-level similarities within multivariate time series data.

3.1 Variational Auto Encoder

We briefly introduce the variational auto-encoder (VAE) [12], which is the base model of StackVAE. VAE is a deep generative model that characterizes the relationship between the input data sample \mathbf{x} and its corresponding latent code \mathbf{z} . Usually we assign a standard Gaussian distribution $p(\mathbf{z}) = \mathcal{N}(\mathbf{0}, \mathbf{I})$ to the latent code \mathbf{z} as its prior distribution. A VAE model is composed of two parts — a decoder network $p(\mathbf{x}|\mathbf{z})$ for generating observations by conditioning on the latent code and an encoder network $q(\mathbf{z}|\mathbf{x})$ for inferring the distribution of latent code for each individual input. In VAE,

the encoder network is needed as an approximation to the intractable posterior distribution $p(\mathbf{z}|\mathbf{x})$ under the framework of variation inference, and it is usually assumed to be multivariate Gaussian distribution $q(\mathbf{z}|\mathbf{x}) = \mathcal{N}(\boldsymbol{\mu}_z, \boldsymbol{\sigma}_z^2 \mathbf{I})$. Then, the parameters of the encoder and decoder networks are jointly optimized by maximizing the evidence lower bound (ELBO):

$$J = \mathbb{E}_{q(\mathbf{z}|\mathbf{x})} [\log p(\mathbf{x}|\mathbf{z})] - \text{KL}(q(\mathbf{z}|\mathbf{x})||p(\mathbf{z})). \quad (1)$$

The common strategy of stochastic gradient descent (SGD) has been extended to solve this problem with promising performance.

3.2 Stacking Block-Wise VAE Model

The stacking block-wise VAE reconstruction model builds a single-channel block-wise reconstruction and stacks it multiple times with a weight-sharing technique (Fig. 2c). Specifically, we define the input slice $X = [\mathbf{x}_1, \dots, \mathbf{x}_N]^\top$ and the reconstruction output $\hat{X} = [\hat{\mathbf{x}}_1, \dots, \hat{\mathbf{x}}_N]^\top$, where \mathbf{x}_n and $\hat{\mathbf{x}}_n$ correspond to the series data of channel n . The latent code of \mathbf{x}_n is defined as \mathbf{z}_n . By stacking \mathbf{z}_n of all channels using the same model, we get the latent code $Z = [\mathbf{z}_1, \dots, \mathbf{z}_N]^\top$ of the slice X .

The encoding process of our model maps the slice X to its posterior latent distribution $q(Z|X)$. For each channel in a slice, $\mathbf{x}_n \in \mathbb{R}^l$ (one row of $X \in \mathbb{R}^{N \times l}$), the encoder of the standard VAE module maps \mathbf{x}_n into the corresponding posterior Gaussian distribution:

$$q(\mathbf{z}_n|\mathbf{x}_n) = \mathcal{N}(\boldsymbol{\mu}_{z_n}, \boldsymbol{\sigma}_{z_n}^2 \mathbf{I}), \quad n = 1, \dots, N, \quad (2)$$

where \mathbf{z}_n has m dimensions, $\boldsymbol{\mu}_{z_n}$ and $\boldsymbol{\sigma}_{z_n}$ represent the means and standard deviations of m independent Gaussian components in \mathbf{z}_n and \mathbf{I} is an identity matrix. Thus the approximated posterior latent distribution for the slice X , i.e., $q(Z|X)$, is obtained with each component $q(\mathbf{z}_n|\mathbf{x}_n)$ identified. Then we randomly sample from $q(\mathbf{z}_n|\mathbf{x}_n)$ to get the latent code \mathbf{z}_n for each channel. The complete encoding procedure is formulated as follows:

$$\begin{aligned} & \text{for } n = 1, \dots, N: \quad \mathbf{h}_{n,1} = f(\mathbf{x}_n), \\ & H_1 = [\mathbf{h}_{1,1}, \dots, \mathbf{h}_{N,1}]^\top, \\ & H_2 = (1 - \gamma)H_1 + \gamma \tilde{A} \times H_1, \\ & \text{for } n = 1, \dots, N: \quad \begin{cases} \boldsymbol{\mu}_{z_n} = f(\mathbf{h}_{n,2}), \\ \boldsymbol{\sigma}_{z_n} = \text{SoftPlus}[f(\mathbf{h}_{n,2})], \end{cases} \end{aligned} \quad (3)$$

where f is a neural linear layer shared among different channels, $\mathbf{h}_{n,2}$ is a row of H_2 (i.e., $H_2 = [\mathbf{h}_{1,2}, \dots, \mathbf{h}_{N,2}]^\top$), and \tilde{A} is a sparse channel-interrelation square matrix obtained by the graph learning module, which will be introduced in the next subsection.

With the neighbours and corresponding interrelation coefficients provided in \tilde{A} , the intermediate latent feature of channel n : $\mathbf{h}_{n,2}$ retains its original state $\mathbf{h}_{n,1}$ with the ratio $1 - \gamma$, while shares the information propagated from its neighbours with the ratio γ . If γ is set as 0, StackVAE will degenerate to the model without the graph learning module. In such a design of the architecture, StackVAE adopts a more robust block-wise model and reduces the model size via the weight sharing technique. As we shall see in experiments, StackVAE derives an effective reconstruction for the time series anomaly detection problem.

The decoder works like the inverse procedure of the encoder, that is, for $n = 1, \dots, N$:

$$\begin{aligned} & \hat{\mathbf{h}}_n = f(\mathbf{z}_n), \\ & \boldsymbol{\mu}_{\hat{\mathbf{x}}_n} = f(\hat{\mathbf{h}}_n), \\ & \boldsymbol{\sigma}_{\hat{\mathbf{x}}_n} = \text{SoftPlus}[f(\hat{\mathbf{h}}_n)] \end{aligned} \quad (4)$$

where $\hat{\mathbf{h}}_n$ denotes the intermediate latent feature, and $\boldsymbol{\mu}_{\hat{\mathbf{x}}_n}$ and $\boldsymbol{\sigma}_{\hat{\mathbf{x}}_n}$ represent the mean and variance of the normal distribution for generating \mathbf{x}_n , respectively:

$$p(\mathbf{x}_n|\mathbf{z}_n) = \mathcal{N}(\boldsymbol{\mu}_{\hat{\mathbf{x}}_n}, \boldsymbol{\sigma}_{\hat{\mathbf{x}}_n}^2 \mathbf{I}). \quad (5)$$

With the individual components $p(\mathbf{x}_n|\mathbf{z}_n)$ for channel n , we can get the overall generating distribution $p(X|Z)$ by multiplying all components together.

In practice, $\boldsymbol{\mu}_{\hat{\mathbf{x}}_n}$ can be adopted as the reconstruction output $\hat{\mathbf{x}}_n$. By stacking $\hat{\mathbf{x}}_n$, we get the reconstruction output $\hat{X} = [\hat{\mathbf{x}}_1, \dots, \hat{\mathbf{x}}_N]^\top$.

3.3 Graph Learning Module

We now design a graph neural network module through the adjacency matrix \tilde{A} in Eqn. 3 to represent the interrelation structure information among the multiple channels of the time-series. Specifically, we regard the channels as the nodes and learn an undirected graph from the representation of each channel data via the following graph neural networks:

$$\begin{aligned} M &= \tanh(\alpha f(E)), \\ A &= \text{ReLU}(\alpha \tanh(MM^\top)), \end{aligned} \quad (6)$$

where E denotes the randomly initialized node embedding for channels and α is an amplifier parameter that controls the saturation rate of the activation function (\tanh and ReLU). Compared with the previous graph learning for the time-series forecasting task [26], our model focuses on the anomaly detection task and aims at learning a time-invariant graph for the stable relationships of normal running states in the probabilistic VAE framework. Moreover, for simplicity, we use the undirected graph, while [26] adopted a directed graph to characterize the directed temporal effect from one channel to another channel.

To ensure the sparsity of the adjacency matrix A , we only retain the top- k values per row and set the others to be zeros. The output \tilde{A} is formulated as follows: for $n = 1, 2, \dots, N$:

$$\begin{aligned} idx &= \text{argtopk}(A[n, :]) \\ A[n, -idx] &= 0 \\ D &= \text{diag} \left[1 + \sum_{j=1}^N A_{1j}, \dots, 1 + \sum_{j=1}^N A_{Nj} \right] \\ \tilde{A} &= D^{-1}(I + A) \end{aligned} \quad (7)$$

where the function argtopk returns the indices of the top- k values in a 1-D tensor, $-idx$ represents the complement set of idx containing indexes of the other $N - k$ values and diag converts a $1 \times N$ tensor into an $N \times N$ diagonal matrix.

We propose a regression-based graph learning loss for graph structure learning, which discovers the stable structure for detection tasks:

$$\mathcal{L}_{\text{Graph}} = \|X - \tilde{A} \times X\|_2^2. \quad (8)$$

where X represents the input slice and \tilde{A} is the output adjacency matrix. The graph learning loss forces the learned adjacency matrix \tilde{A} to characterize the stable working states of monitored devices from the view of the linear regression, which shares the thought of lasso [27], the classical structure learning approach. Differently, the sparsity of structure is achieved by retaining the top- k neighbours, instead of the L1-regularization. When the data of different channels are independent, we can learn the extreme case that \tilde{A} is an identity matrix and $\mathcal{L}_{\text{Graph}} = 0$.

With the combinations of rows in the mid-latent feature H_1 , the latent feature in the next layer H_2 involves interrelation structure information among channels. Intuitively, when we use H_1 to calculate the embedding of the next layer H_2 , we propagate the information over highly-correlated nodes. With the graph learning loss, the interrelated neighbours contribute to the encoding process of one certain channel with different weights according to the learned interpretable interrelation graph structure. The sparsity of the interrelation outputs benefits the interpretability of the multi-channel reconstruction model.

3.4 Loss Function

The StackVAE's learning objective is the same as VAE's, that is to maximize the evidence lower bound (ELBO), which is equivalent to minimizing the following loss function:

$$\mathcal{L}_{\text{VAE}} = -\mathbb{E}_{q(Z|X)}[\log p(X|Z)] + \text{KL}(q(Z|X)||p(Z)) \quad (9)$$

Collaborating with the graph learning loss introduced in Section 3.3, the complete form of StackVAE-G's loss function is given below:

$$\begin{aligned} \mathcal{L}_{\text{total}} &= \mathcal{L}_{\text{VAE}} + \lambda \mathcal{L}_{\text{Graph}} \\ &= -\mathbb{E}_{q(Z|X)}[\log p(X|Z)] + \text{KL}(q(Z|X)||p(Z)) \\ &\quad + \lambda \|X - \tilde{A} \times X\|_2^2 \end{aligned} \quad (10)$$

where λ is a hyper-parameter to balance the two parts of the loss functions.

3.5 Training & Detecting Procedures

For training, the two modules of StackVAE-G, namely the StackVAE model and the graph learning module, are jointly trained by optimizing $\mathcal{L}_{\text{total}}$ in Eqn. 10 using Adam [28]. The encoder of StackVAE together with the graph learning module is trained to infer the true posterior latent distribution $p(X|Z)$ with interpretable interrelation among channels. After random sampling from the approximated posterior $q(Z|X)$, the decoder is trained to accurately generate the reconstruction outputs \hat{X} . After training for several epochs, the random sampling process guarantees the continuous space formed by these Z samples is linked to the normal pattern of input X .

For detection, with the reconstructed normal pattern $\hat{X} = [\hat{x}_1, \dots, \hat{x}_N]^\top$ for input X , the anomaly score of each time step t in X is defined as the sum of the squared error between original inputs and reconstruction outputs:

$$s_t = \sum_{n=1}^N (\hat{x}_{n,t} - x_{n,t})^2 \quad (11)$$

where $x_{n,t}$ represents the value of \hat{x}_n at time step t and $\hat{x}_{n,t}$ is the reconstruction value of $x_{n,t}$. After getting the anomaly scores, we select a constant threshold c . Then the time step t with $s_t > c$ will be considered as an anomalous point. Though we may calculate the score for each time step in one slice X , when performing online detection we only use the score of the last point for a quick real-time response. For the detection outputs, anomalies often occur in the form of continuous anomalous segments. And once an alert is triggered within the lasting period of an anomaly, this anomalous segment is considered to be detected. We adopt the point-adjust evaluation approach [8] which recognize a correct detection if any point in this segment is detected.

4 Experiments

We now present the experimental results of StackVAE-G on various datasets by comparing with state-of-the-art baselines.

Table 1: Performance Comparison

Methods	SMD			SMAP			MSL		
	P	R	F1	P	R	F1	P	R	F1
IF	0.5938	0.8532	0.7003	0.4423	0.5105	0.4739	0.5681	0.6740	0.6166
LSTM-VAE	0.8698	0.7879	0.8268	0.7164	0.9875	0.8304	0.8599	0.9756	0.9141
DAGMM	0.6730	0.8450	0.7493	0.6334	0.9984	0.7751	0.7562	0.9803	0.8537
LSTM-NDT	0.5684	0.6438	0.6037	0.8965	0.8846	0.8905	0.5934	0.5374	0.5640
OmniAnomaly	0.9809	0.9438	0.9620	0.7585	0.9756	0.8535	0.9140	0.8891	0.9014
USAD	0.9314	0.9617	0.9463	0.7697	0.9831	0.8634	0.8810	0.9786	0.9272
StackVAE+Fixed Graph	0.9616	0.9472	0.9543	0.8932	0.9315	0.9119	0.7704	0.9825	0.8636
StackVAE	0.9605	0.9469	0.9536	0.8948	0.9315	0.9128	0.8999	0.9955	0.9453
StackVAE-G	0.9561	0.9538	0.9550	0.9014	0.9310	0.9160	0.9172	0.9955	0.9547

4.1 Data and Evaluation Metrics

We conduct our experiments on three public datasets, as detailed below:

- **Server Machine Dataset (SMD):** SMD is published by [9], which lasts for 5 weeks long, monitors 28 server machines for a large Internet company with 33 sensors. SMD is the largest public dataset currently available for evaluating multivariate time-series anomaly detection. It contains metrics like CPU load, network usage, memory usage, etc.
- **Soil Moisture Active Passive (SMAP) satellite and Mars Science Laboratory (MSL) rover Datasets:** SMAP and MSL are two datasets published by NASA [10]. SMAP contains 55 entities and each entity is monitored by 25 sensors. MSL contains 27 entities and 66 sensors for each entity. The metrics in the two datasets include telemetry data, radiation, temperature, power, computational activities, etc [9].

We use a max-min pre-processing to transfer the raw data to $[0, 1]$ [7]. And we use *precision* (P), *recall* (R), and *F1 score* (F1) as the evaluation metrics.

4.2 Baseline Methods

StackVAE-G is the proposed method to be evaluated and we also include the following variations into comparisons:

- *StackVAE*: the StackVAE-G model with $\gamma = 0$ (i.e., omitting the graph learning module);
- *StackVAE+Fixed Graph*: a two-stage model which firstly learns the graph structure with the lasso regression and then uses the fixed structure in the stacking block-wise reconstruction framework for detection.

We select six state-of-the-art unsupervised models for multivariate time-series anomaly detection as our baselines, including *Isolation Forest* [19] (IF), *LSTM-VAE* [7], *Deep Autoencoding Gaussian Mixture Model* (DAGMM) [29], *LSTMs with Nonparametric Dynamic Thresholding* (LSTM-NDT) [10], *OmniAnomaly* [9], and *Unsupervised Anomaly Detection* (USAD) for multivariate time-series [14]. For each model, we test its possible anomaly thresholds and report its best performance according to the metric of F1-score, which is consistent with [14]. We use the lasso regression for each channel as a qualitative baseline to compare the learned interrelation graph structure. Let the data of channel n : \mathbf{x}_n be the target and the other channels $\mathbf{x}_{-n} = [\mathbf{x}_1, \mathbf{x}_2, \dots, \mathbf{x}_{n-1}, \mathbf{x}_{n+1}, \dots, \mathbf{x}_N]^\top$ be the predictors. The lasso regression aims to find the regression coefficients $\beta_n \in \mathbb{R}^{N-1}$:

$$\beta_n = \arg \min_{\beta} \left\{ \mathbb{E}_t \left[\frac{1}{2} |\beta_n^\top \mathbf{x}_{-n,t} - x_{n,t}|^2 \right] + \lambda \|\beta_n\|_1 \right\}. \quad (12)$$

We solve Eqn. 12 for each channel from \mathbf{x}_1 to \mathbf{x}_N . Note that β_n contains $N - 1$ coefficients for \mathbf{x}_{-n} regard less of \mathbf{x}_n itself, it is equivalent to add \mathbf{x}_n as a predictor with the regression coefficient 0. Thus we obtain $\hat{\beta}_n \in \mathbb{R}^N$ with $\hat{\beta}_{n,n} = 0$. Finally we learn the regression coefficient matrix $A = [\hat{\beta}_1, \hat{\beta}_2, \dots, \hat{\beta}_N]^\top$. Following the process in Eqn. 7, we calculate D and then get the final output $\tilde{A} = D^{-1}(I + A)$.

4.3 Hyper-parameters for StackVAE-G

There are four hyper-parameters for the graph learning module, which are chosen via the grid search:

- *Fusion ratio*: The parameter γ in (Eqn. 3) controls the ratio of fused mid-latent feature $\tilde{A} \times H_1$ in H_2 . We search it in the range $[0.1, 1.0]$ with 0.1 as the step size. The detection performance fluctuates mildly and gets the best performance around 0.5, which indicates that the fusion process among channels is beneficial while the original features of each channel also need to be protected.
- *Amplifier*: we use α to represent the amplifier parameter as in Eqn. 6. The larger α is, the more relevant neighbours can be found. If the amplifier is set to be 0, apparently the learned graph structure \tilde{A} will be an identity matrix \mathbf{I} with no neighbours found. And this hyper-parameter is insensitive because as the graph learning loss converges, only the highly-correlated channels are still connected. The larger amplifier provides more neighbour candidates and the graph learning loss decides which can stay. We search it in the range $[1.0, 2.5]$ with 0.1 as the step size, and get the best structure learning performance at 2.0.
- *Top-k*: to ensure the sparsity of the graph, k is set to mask the other elements in a row of \tilde{A} except the top- k elements. When setting the value of k , we need to make sure that k is comparable with the size of the largest cluster of nodes, so that the interrelation structure learned can reveal the complete information. k is selected in the set $\{5, 10, 15, 20\}$ and differs in different datasets.
- *Hyper-parameter for loss function*: we set a hyper-parameter λ to balance the two parts of StackVAE-G's loss function. We search it in the range $[0.5, 2.0]$ with 0.5 as the step size.

The selection of all hyper-parameters is detailed in Appendix A.

4.4 Analysis on Numerical Results

Table 1 shows the detailed performance report for all selected approaches on three public datasets. The performance of the six baselines is cited from [9, 14]. Owing to the stacking reconstruction model and the graph learning module, StackVAE-G (and its variations) outperforms all the other methods on aerospace datasets SMAP and MSL with considerable improvements (lifting the F1-scores by 0.0526 and 0.0275, compared with the newly-proposed USAD), firstly breaking the record of LSTM-NDT on SMAP. And it is the second best on SMD, further narrowing the gap with

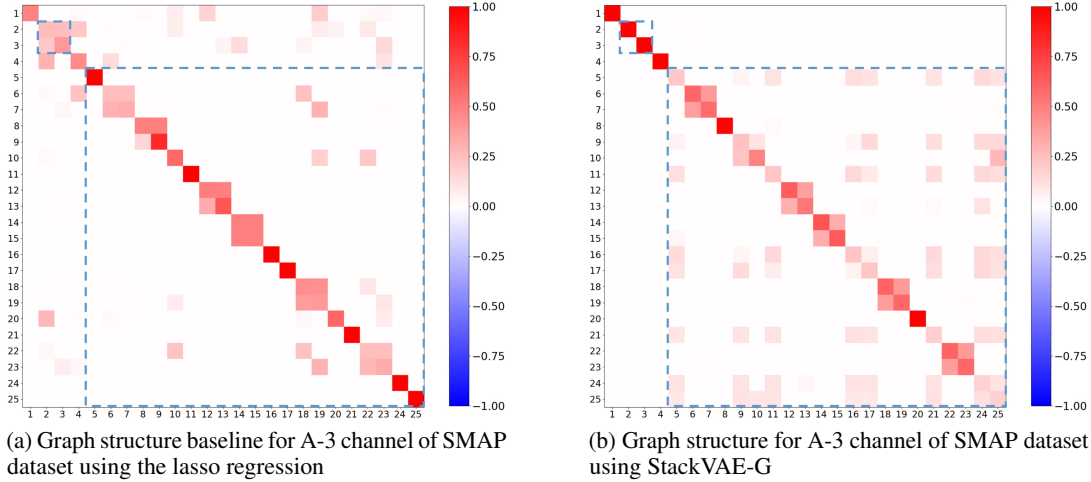


Figure 4: Comparison between the graph structures learned by the lasso regression and StackVAE-G. The Row (Column) n is corresponding to channel n of the multivariate time-series data. The colored pixels in Row (Column) n represents the neighbours of channel n . The lasso regression fails to learn accurate graph structure due to wrong connection between channel 2,3 and failures among zero-composed channels 5, 11, 16, 17, 21, 24 and 25. StackVAE-G avoids these failures and mistakes, revealing intuitive clustering information among channels.

OmniAnomaly. The detection performance indicates its effectiveness for multivariate time series anomaly detection task with channel-level similarities considered. IF and DAGMM present the relatively lower performance because they do not consider the temporal information of the time-series data.

As for the StackVAE model variations, StackVAE-G with the graph neural network module shows a comparable or slightly better detection result compared with StackVAE, the one without the graph learning module. Moreover, StackVAE-G also has a better detection result compared with the StackVAE+Fixed Graph method, which reveals that StackVAE-G successfully models the graph structure in the VAE generative modeling.

Table 2: Average performance of StackVAE-G (\pm standard deviation) on each dataset

Datasets	Precision	Recall	F1-score
SMD	0.9541(0.0015)	0.9544(0.0010)	0.9542(0.0007)
SMAP	0.8983(0.0022)	0.9310(0.0000)	0.9143(0.0011)
MSL	0.9084(0.0053)	0.9955(0.0000)	0.9500(0.0029)

Additionally, to demonstrate the stable detection performance of StackVAE-G, we repeat the training and testing procedures for 5 times individually and report the average performance metrics with the corresponding standard deviations. From Table 2, we can see the average performance is quite close to the best shown in Table 1 and the standard deviations are quite small.

4.5 Analysis on Training Time

We report the average time cost per epoch for one instance in each dataset and the involved methods are StackVAE-G and other two strong baselines, *OmniAnomaly* and USAD. The training time of *OmniAnomaly* and USAD is cited from [14]. As can be seen in Table. 3, StackVAE-G is more efficient compared with *OmniAnomaly* and has a comparable efficiency with USAD (on SMAP and MSL, the training efficiency is further improved). All methods are trained on one NVIDIA GeForce GTX 1080 Ti.

As can be seen in Fig. 2, when fixing the same window size, the model size of the stacking block-wise model with the weight-sharing technique is smaller compared with the previous step-wise and block-wise models, which results in its better training efficiency. Besides, the graph learning module has a limited impact on the overall model efficiency.

4.6 Analysis on Graph Structure

In Fig. 4, we plot the heat maps of the adjacency matrices learned from the A-3 instance of the SMAP dataset to show the graph structure. The left subplot represents the graph structure learned by the lasso regression, while the result of StackVAE-G is shown on the right. We focus on finding the highly-correlated neighbours for each channel and sharing their normal patterns within each group. We can see that both methods discover the similarities between channel (6, 7),

Table 3: Training Time per epoch (min)

Methods	SMD	SMAP	MSL
OmniAnomaly	87	48	11
USAD	0.06	0.08	0.03
StackVAE-G	0.127	0.013	0.012

(18, 19) and (22, 23), while StackVAE-G succeeds in finding the most related neighbours (e.g., the all-zeros channels 5, 11, 16, 17, 21, 24, and 25, as illustrated in Fig. 1), so as to give a reliable and accurate graph structure. Moreover, in the graph structure of the lasso regression, some irrelevant channels are connected. For example, channels 2 and 3 have totally different curves.

We also give an ablation study of the StackVAE-G by removing the graph learning loss in Eqn. 8. The results are shown in Fig. 5. We can see that without supervision on graph learning, the graph structure learned is completely uninterpretable and cannot match the curves shown in Fig. 1. It implies that the graph learning loss indeed helps StackVAE-G to correctly learn the stable and reliable graph structure.

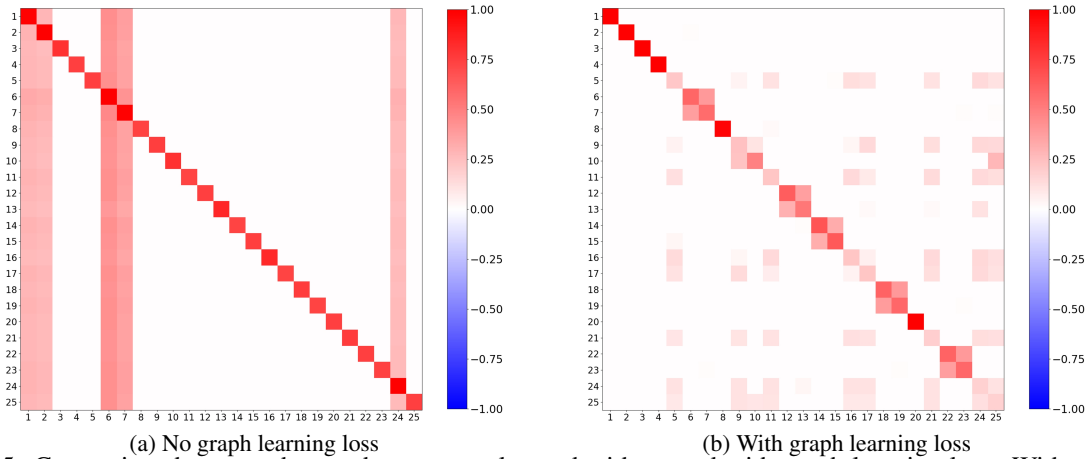


Figure 5: Comparison between the graph structures learned without and with graph learning loss. Without graph learning loss, StackVAE-G fails to learn meaningful graph structure, indicating transferring the graph learning module from prediction tasks [26] directly doesn’t work under stacking block-wise reconstruction framework. graph learning loss ensures that StackVAE-G can learn meaningful and stable graph structure.

5 Conclusion and discussion

In this paper, we propose a stacking VAE model with graph neural networks for effective and interpretable time-series anomaly detection. To this end, we propose a stacking block-wise reconstruction framework with a weight-sharing technique to exploit the channel-level similarities within multivariate time series data, which can effectively reconstruct the normal series patterns. To exploit the interrelation structure information among the multiple channels, our model learns a sparse adjacency matrix using a graph learning module from each channel of time-series data. Collaborating with the graph learning loss, the graph learning module learns the stable graph structure with high quality. Furthermore, we use the interrelation structure information for interpretable reconstruction of normal series patterns. We conduct experiments on three commonly-used multivariate time-series anomaly detection datasets, SMD, SMAP, and MSL. Our proposed model outperforms the strong baselines on detection performance with considerable improvements. Furthermore, the training time comparison shows that the proposed method is relatively more efficient when training, which strengthens the applicability for the real-world time series anomaly detection tasks. When the StackVAE-G model is trained for a time series anomaly detection problem, the user or the operator takes the following steps to take the model outputs into account. First run the model to test the coming time series streams and decide whether an anomaly occurs. When an anomaly occurs, the operator can check the learned graph output adjacency matrix to get the interrelated neighbours of each channel. Either with or without the prior knowledge for the certain problem, the human operator can easily perform the failure diagnosis to see whether it is a sensor clerical error or a systematic error, which corresponds to a single-channel anomaly and a structural multi-channel anomaly respectively. Therefore, our model outputs can provide useful interpretability for better system failure diagnosis.

The interrelation structure we study in this paper is linear (See $\mathcal{L}_{\text{Graph}}$ in Eqn. 8), which commonly exists in many applications. But the designed graph learning objective $\mathcal{L}_{\text{Graph}}$ is unable to describe the relationship between two variables like $y = x^2$ and other non-linear relationships. We leave it as a future work.

References

- [1] Charu Aggarwal. *Outlier Analysis*. Springer, 2015.
- [2] Guansong Pang, Chunhua Shen, Longbing Cao, and Anton van den Hengel. Deep learning for anomaly detection: A review. *CoRR*, abs/2007.02500, 2020.
- [3] Leonid Portnoy, Eleazar Eskin, and Sal Stolfo. Intrusion detection with unlabeled data using clustering. In *ACM CSS Workshop on Data Mining Applied to Security (DMSA-2001)*, pages 5–8, 2001.
- [4] Yufeng Kou, Chang-Tien Lu, Sirirat Sirwongwattana, and Huang Yo-Ping. Survey of fraud detection techniques. In *Networking, sensing and control*, volume 2, pages 749–754, 2004.
- [5] Weng-Keen Wong, Andrew W. Moore, Gregory F. Cooper, and Michael M. Wagner. Bayesian network anomaly pattern detection for disease outbreaks. In Tom Fawcett and Nina Mishra, editors, *Machine Learning, Proceedings of the Twentieth International Conference (ICML 2003), August 21-24, 2003, Washington, DC, USA*, pages 808–815. AAAI Press, 2003.
- [6] Andrew Lerner. Aiops platforms, August 2017.
- [7] D. Park, Y. Hoshi, and C. C. Kemp. A multimodal anomaly detector for robot-assisted feeding using an lstm-based variational autoencoder. *IEEE Robotics and Automation Letters*, 3(3):1544–1551, 2018.
- [8] Haowen Xu, Wenxiao Chen, Nengwen Zhao, Zeyan Li, Jiahao Bu, Zhihan Li, Ying Liu, Youjian Zhao, Dan Pei, Yang Feng, Jie Chen, Zhaogang Wang, and Honglin Qiao. Unsupervised anomaly detection via variational auto-encoder for seasonal kpis in web applications. In *Proceedings of the 2018 World Wide Web Conference on World Wide Web*, 2018.
- [9] Ya Su, Youjian Zhao, Chenhao Niu, Rong Liu, Wei Sun, and Dan Pei. Robust anomaly detection for multivariate time series through stochastic recurrent neural network. In Ankur Teredesai, Vipin Kumar, Ying Li, Rómer Rosales, Evimaria Terzi, and George Karypis, editors, *Proceedings of the 25th ACM SIGKDD International Conference on Knowledge Discovery & Data Mining*, pages 2828–2837, 2019.
- [10] Kyle Hundman, Valentino Constantinou, Christopher Laporte, Ian Colwell, and Tom Söderström. Detecting spacecraft anomalies using lstms and nonparametric dynamic thresholding. In Yike Guo and Faisal Farooq, editors, *Proceedings of the 24th ACM SIGKDD International Conference on Knowledge Discovery & Data Mining*, pages 387–395, 2018.
- [11] Geoffrey E. Hinton, Simon Osindero, and Yee Whye Teh. A fast learning algorithm for deep belief nets. *Neural Computation*, 18(7):1527–1554, 2006.
- [12] Diederik P. Kingma and Max Welling. Auto-encoding variational bayes. In Yoshua Bengio and Yann LeCun, editors, *2nd International Conference on Learning Representations, ICLR 2014, Banff, AB, Canada, April 14-16, 2014, Conference Track Proceedings*, 2014.
- [13] Pankaj Malhotra, Anusha Ramakrishnan, Gaurangi Anand, Lovekesh Vig, Puneet Agarwal, and Gautam M. Shroff. Lstm-based encoder-decoder for multi-sensor anomaly detection. *CoRR*, abs/1607.00148, 2016.
- [14] Julien Audibert, Pietro Michiardi, Frédéric Guyard, Sébastien Marti, and Maria A. Zuluaga. USAD: unsupervised anomaly detection on multivariate time series. In Rajesh Gupta, Yan Liu, Jiliang Tang, and B. Aditya Prakash, editors, *KDD '20: The 26th ACM SIGKDD Conference on Knowledge Discovery and Data Mining, Virtual Event, CA, USA, August 23-27, 2020*, pages 3395–3404. ACM, 2020.
- [15] Chuxu Zhang, Dongjin Song, Yuncong Chen, Xinyang Feng, Cristian Lumezanu, Wei Cheng, Jingchao Ni, Bo Zong, Haifeng Chen, and Nitesh V. Chawla. A deep neural network for unsupervised anomaly detection and diagnosis in multivariate time series data. In *The Ninth AAAI Symposium on Educational Advances in Artificial Intelligence, EAAI 2019, Honolulu, Hawaii, USA, January 27 - February 1, 2019*, pages 1409–1416, 2019.
- [16] Yifan Guo, Weixian Liao, Qianlong Wang, Lixing Yu, Tianxi Ji, and Pan Li. Multidimensional time series anomaly detection: A gru-based gaussian mixture variational autoencoder approach. In *Proceedings of The 10th Asian Conference on Machine Learning*, 2018.
- [17] Charu C. Aggarwal. *Supervised Outlier Detection*, pages 169–198. Springer New York, New York, NY, 2013.
- [18] Larry M. Manevitz and Malik Yousef. One-class svms for document classification. *J. Mach. Learn. Res.*, 2:139–154, 2001.

- [19] Fei Tony Liu, Kai Ming Ting, and Zhi-Hua Zhou. Isolation forest. In *Proceedings of the 8th IEEE International Conference on Data Mining (ICDM 2008), December 15-19, 2008, Pisa, Italy*, pages 413–422. IEEE Computer Society, 2008.
- [20] Danilo Jimenez Rezende and Shakir Mohamed. Variational inference with normalizing flows. In Francis R. Bach and David M. Blei, editors, *Proceedings of the 32nd International Conference on Machine Learning, ICML 2015, Lille, France, 6-11 July 2015*, volume 37 of *JMLR Workshop and Conference Proceedings*, pages 1530–1538. JMLR.org, 2015.
- [21] James Douglas Hamilton. *Time series analysis*. Princeton university press, 2020.
- [22] Sepp Hochreiter and Jürgen Schmidhuber. Long short-term memory. *Neural computation*, 9(8):1735–1780, 1997.
- [23] Zou and Hui. The adaptive lasso and its oracle properties. *Publications of the American Statist Association*, 101(476):1418–1429, 2006.
- [24] Francis R Bach and Michael I Jordan. Learning graphical models for stationary time series. *IEEE transactions on signal processing*, 52(8):2189–2199, 2004.
- [25] Jerome Friedman, Trevor Hastie, and Robert Tibshirani. Sparse inverse covariance estimation with the lasso, 2007.
- [26] Zonghan Wu, Shirui Pan, Guodong Long, Jing Jiang, Xiaojun Chang, and Chengqi Zhang. Connecting the dots: Multivariate time series forecasting with graph neural networks. In Rajesh Gupta, Yan Liu, Jiliang Tang, and B. Aditya Prakash, editors, *KDD '20: The 26th ACM SIGKDD Conference on Knowledge Discovery and Data Mining, Virtual Event, CA, USA, August 23-27, 2020*, pages 753–763. ACM, 2020.
- [27] Nicolai Meinshausen and Peter Bühlmann. High-dimensional graphs and variable selection with the lasso. *The Annals of Statistics*, 34(3):1436–1462, Jun 2006.
- [28] Diederik P. Kingma and Jimmy Ba. Adam: A method for stochastic optimization. In Yoshua Bengio and Yann LeCun, editors, *3rd International Conference on Learning Representations, ICLR 2015, San Diego, CA, USA, May 7-9, 2015, Conference Track Proceedings*, 2015.
- [29] Bo Zong, Qi Song, Martin Renqiang Min, Wei Cheng, Cristian Lumezanu, Dae-ki Cho, and Haifeng Chen. Deep autoencoding gaussian mixture model for unsupervised anomaly detection. In *6th International Conference on Learning Representations, ICLR 2018, Vancouver, BC, Canada, April 30 - May 3, 2018, Conference Track Proceedings*, 2018.

A Hyper-parameters

Table 4 shows the hyper-parameters selected for different datasets. Note that besides the above four hyper-parameters, StackVAE-G have another two — window size l and the dimension of latent space m . StackVAE and StackVAE-G share the parameters l and m .

Table 4: Hyper-Parameters Settings

Datasets	StackVAE		StackVAE-G			
	l	m	γ	k	α	λ
SMD	40	20	0.5	10	2.0	1.0
SMAP, MSL	100	20	0.5	15	2.0	1.0

The other parameters for model training are listed in Table 5. They are the same for both StackVAE and StackVAE-G.

Table 5: The Other Parameters

Other Parameters For Training	
Optimizer	Adam [28]
learning rate	1e-3
learning rate decay	0.8
weight decay	1e-3
gradient clip value	12.0
epochs	256
batch size	64